Brazilian Journal
of Chemical
Engineering

ISSN 0104-6632
Printed in Brazil
www.scielo.br/bjce

CC BY

Vol. 35, No. 01, pp. 217 – 228, January – March, 2018
dx.doi.org/10.1590/0104-6632.20180351s20150595

HARMONIOUS INTERACTION OF INCORPORATING CNTs AND ZEOLITIC IMIDAZOLE FRAMEWORKS INTO POLYSULFONE TO PREPARE HIGH PERFORMANCE MMMS FOR CO_2 SEPARATION FROM HUMIDIFIED POST COMBUSTION GASES

Muhammad Sarfraz [1,2] and M. Ba-Shammakh[2,*]

[1] Department of Polymer and Process Engineering, University of Engineering and Technology, Lahore-Pakistan
[2] Department of Chemical Engineering, King Fahd University of Petroleum and Minerals, Dhahran- KSA,
P.O. Box 5050, Postal Code 31261.

(Submitted: October 19, 2015; Revised: April 15, 2016; Accepted: June 8, 2016)

Abstract – Multi-walled carbon nanotubes (CNTs) and zeolitic imidazole frameworks (ZIF-301) were synergistically incorporated into glassy polysulfone (PSF) to prepare mixed-matrix membranes (MMMs) to separate CO_2 from post combustion flue gas. The flexible MMMs rendering consistent distribution and improved adhesion of nanofillers with the polymer matrix were hydrothermally stable under wet conditions. Gas sorption analysis along with dry and wet gas permeation experiments showed that both CO_2 permeability and CO_2/N_2 selectivity of MMMs were improved owing to the synergistic effect of nanofillers. The MMM filled with 18 wt % ZIF-301 nanofillers and 6 wt % CNTs showed an optimum separation performance by providing a CO_2 permeability of 19 Barrers with a CO_2/N_2 selectivity of 48. The CO_2 separation performance of MMMs prepared in this work was found to be better than those of already existing hydrothermally stable MMMs.

Keywords: Hydrophobic MMMs, ZIF-301, CNTs, CO_2 capture, permselectivity

INTRODUCTION

CO_2 emissions from burning of fossil fuels induce environmental warming concerns throughout the globe (D'Alessandro *et al.*, 2010; Jacobson, 2009; MacDowell *et al.*, 2010). Economically viable processes to reduce CO_2 releases include its sequestration or capture from a mixture of CO_2-containing gases (Herzog and Golomb, 2004; Hussain and Hägg, 2010). On account of its flexible design, ease of scale up, high efficiency, low energy requirement, simple function, low capital and operating costs, and environmental friendliness, polymer-based mixed-matrix membrane gas separation technology, among other conventional processes, has gained momentous attention (Zhao *et al.*, 2006; Pandey and Chauhan, 2011; ahajan and Koros, 2000; Fawas *et al.*, 2007; Baker, 2002; Gin and Noble, 2011; Xiao and Chung, 2011; Staudt-Bickel and Koros, 1999).

Majority of glassy polymers have been adapted to fabricate MMMs by adding inorganic fillers like nonporous silica (Merkel *et al.*, 2002; Ahn *et al.*, 2008), structured mesoporous silica (Reid *et al.*, 2011; Kim *et al.*, 2006; Kim

* *Corresponding Author*: M. Ba-Shammakh. E-mail: shammakh@kfupm.edu.sa; Phone: +966138602205

and Marand, 2008), carbon molecular sieves (Vu *et al.*, 2003), carbon nanotubes (Cong *et al.*, 2007; Kim *et al.*, 2007), zeolites (Gorgojo *et al.*, 2008), and microporous metal organic frameworks (MOFs) (Liu *et al.*, 2014) in order to design efficient mix membranes showing better permselectivity characteristics as compared to unfilled polymer membranes. Advantages of adding microporous nanomaterials (such as ZIFs/MOFs and/or CNTs/graphenes etc.) into a polymer matrix to form MMMs comprise the ability to combine the simplicity of casting and processability, enhanced mechanical and chemical performance of polymers conjoined with improved gas separation efficiency of nanocrystals possessing adjustable pore dimensions, modifiable surface functionality, and high surface areas (Harold *et al.*, 2012).

Nanocrystals of microporous zeolitic imidazolate frameworks are interesting materials to fabricate efficient MMMs for gas separation on account of their high surface areas, tunable nano-sized pores, modifiable surface functionality, good wetting characteristics, and improved thermal and chemical stability (Li *et al.*, 2013; Chen *et al.*, 2014; Mohammad *et al.*, 2013). Hydrothermally stable ZIF-301 crystals (Nhung *et al.*, 2014) selectively capture CO_2 gas from $CO_2/N_2/H_2O$ wet gaseous mixture and their inclusion into polymer matrices is expected to improve separation performance of MMMs under wet conditions.

Owing to their internal smooth walls, nano-sized configuration, large pore diameter, high aspect ratio, excellent mechanical and thermal properties (Chen *et al.*, 2006; Sholl *et al.*, 2006; Skoulidas *et al.*, 2006), gas permeation through CNTs is exceptionally higher as compared to other microporous materials. The selectivity of as-synthesized CNTs for various gas molecules is comparatively low and tricky to recover by chemical modification/functionalization due to their inert nature (Kim *et al.*, 2007; Chamberlain *et al.*, 2011; Ismail *et al.*, 2009). Although CNTs-filled MMMs are significantly efficient as compared to MOF/ZIF-based MMMs, good adhesion and uniform dispersion of nanofillers in polymer matrices is the central challenge. A more refined strategy to engineer MMMs with enhanced permselectivity is the synergistic incorporation of naonfillers possessing diversified morphology, nature, and dimensions into a polymer matrix (Ge *et al.*, 2013).

Different types of zeolites (e.g., S1C), MOFs (e.g., HKUST-1), MILs (e.g., NH_2-MIL-53(Al)) and ZIFs (e.g., ZIF-8) were added into PSF to prepare MMMs to study the permeation of CO_2, N_2, CH_4, O_2, and H_2 gases (Zornoza *et al.*, 2011). The CO_2/N_2 permselectivity was not ameliorated for S1C-ZIF-8/PSF MMMs. The CO_2 permeation characteristics of HKUST-1/ZIF-8/PSF, S1C/PSF, HKUST-1/PSF, and ZIF-8/PSF MMMs were found to be 8.4, 9.4, 9.5 and 12.3 Barrers, respectively, with corresponding CO_2/N_2 permselectivities of 38, 23, 24, and 19. The synergistic impact of adding mesoporous silica MCM-41 and amine-functionalized MIL-53(Al) nanofillers into polymer-based MMMs improved their gas separation efficiency (Valero *et al.*, 2013). Galve *et al.* (2013) fabricated hybrid membranes by introducing mesoporous silica MCM-41 spheres and layered microporous titanosilicate JDF-L1 sheets into a glassy polyimide matrix; the uniform distribution of MCM-41 spheres in the polymer matrix was facilitated by JDF-L1 sheets. Li *et al.* (2015) investigated the combined inclusion of graphene oxide and CNTs into PSF to determine optimal loadings of the nanofillers.

The exclusive incorporation of CNTs and ZIFs into a PSF matrix helped to improve the gas separation efficiency of CO_2. The current work focuses on combined inclusion of CNTs and ZIF-301 nanocrystals into a glassy PSF matrix for the first time to fabricate PSF/CNTs/ZIF-301 MMMs to efficiently separate CO_2 from a CO_2/N_2 mixture. The main objective of this study is to develop water-stable composite membranes to efficiently separate CO_2 from humidified post combustion flue gas.

EXPERIMENTAL

Materials

Glassy polysulfone having an average molecular weight of ~35000 by LS and density 1.25 g cm^{-3}, was purchased from Sigma Aldrich. Hydroxyl modified multi-walled CNTs having an average length of 1.2 μm and diameter of 8 nm were obtained from Nanjing XFNANO Materials Tech. Co., Ltd. Zinc nitrate hexahydrate and 2-methylimidazole were obtained from Merck Chemical Company. 5(6)-Chlorobenzimidazole, methanol and N,N-dimethylformamide (DMF) were obtained from Aldrich Chemical Company. All the chemicals and polymer were used as received without further treatment. Highly pure CO_2, N_2 and He gases were used for gas sorption and permeation experiments.

Synthesis of ZIF-301 nanocrystals

ZIF-301 nanocrystals were synthesized by dissolving 67.8 mg of $Zn(NO_3)_2 \cdot 6H_2O$ (the metal salt), 23.4 mg of 2-methylimidazole (primary organic linker), and 43.6 mg of 5(6)-chlorobenzimidazole (secondary organic linker) in a mixture of 9.5 mL DMF and 0.5 mL of distilled water by sonication in a 20-mL vial for 10 minutes. The ensuing solution was then subjected to moderate stirring on a hot plate at 50 °C for 70 hours to obtain a colorless suspension of ZIF-301 nanocrystals. The suspended nanocrystals were separated from the mother liquor by centrifuge and washed with 7 mL of fresh DMF. This process was repeated 5 times to make them ready to prepare MMMs of varying composition.

Preparation of PSF/CNTs/ZIF-301 MMMs

Bare PSF membrane and PSF/CNTs/ZIF-301 MMMs were prepared by degassing the main constituents, i.e., PSF, CNTs and ZIF-301 nanocrystals at 100 °C under vacuum for 20 h to remove adsorbed gases and/or moisture. Bare PSF membrane was prepared by dissolving 1g PSF in 10 mL DMF followed by stirring at room temperature for 24 h until a thick viscous solution was formed. The MMMs containing different amounts of CNTs and ZIF-301 nanocrystals were prepared as follows. 1 g PSF was added in 10 mL DMF and stirred at room temperature for 20 h. Then a weighed quantity of CNTs was dispersed in 4 mL DMF by sonicating for 1 h to get a well dispersed homogeneous suspension. In addition, a specified amount of ZIF-301 nanocrystals was redispersed in 7 mL DMF by stirring for 10 minutes. The three solutions were mixed together and subjected to vigorous stirring for another 12 h until a thick viscous solution was obtained. All the membranes were knife cast on clean glass plates at a specified gate height using a flat sheet membrane casting system (FSMCS). After allowing the solvent to slowly evaporate from the membranes under ambient conditions overnight, the membranes were detached from the glass plates and placed in a VO 200 vacuum oven to dry the MMMs at 80, 100 and 170 °C for 12, 20 and 60 h, respectively, to ensure complete removal of the traces of solvent before subjecting them to gas permeation experiments.

The prepared MMMs were designated as PSF/CNTs(X)/ZIF-301(Y), where X (ranging from 2-10), and Y (ranging from 6-30) represent loadings of CNTs and ZIF-301 by wt %, respectively. As an illustration the MMM denoted by PSF/CNTs(6)/ZIF-301(18) contains 6 and 18 wt % loadings of CNTs and ZIF-301 nanocrystals, respectively. The thicknesses of the membranes were determined in the range of 50-80 μm as measured by a digital micrometer.

Materials Characterization Methods

The measurement techniques used to characterize ZIF-301 nanocrystals, CNTs, bare PSF and PSF/CNTs/ZIF-301 MMMs include X-ray diffraction, scanning electron microscopy, thermal gravimetric analysis, and gas sorption analyses. The volume fraction of nanofillers added in the MMMs can be defined as:

$$\hat{O}_D = \frac{m_D / \rho_D}{m_D / \rho_D + m_C / \rho_C} \times 100 \qquad (1)$$

where m and ρ represent mass and density of PSF (continuous phase denoted by subscript C) and CNTs and/or ZIF-301 nanofillers (dispersed phase denoted by subscript D), respectively. Normally the void volume of MMMs is insignificant as indicated by SEM micrographs and gas sorption analyses. Hence the apparent volume fraction of nanofillers can safely be considered as the true volume fraction of CNTs and/or ZIF-301 nanocrystals collectively doped in MMMs (Song *et al.,* 2012).

Powder X-ray diffraction (XRD) patterns of all the materials were performed using a Bruker D8 X-ray diffractometer using Cu Kα radiation (λ = 1.5406 Å) operated at 45 mA and 40 kV with a step increment of 0.02° in 2θ and a scan size of 0.02° s^{-1}. The membrane samples were loaded in a sample holder placed on a silicon substrate. The MMMs were characterized by XRD to check whether the polymeric matrix alters the crystalline patterns of CNTs and ZIF-301 nanocrystals.

Scanning electron microscopy images were taken to investigate the morphology of MMMs with a Hitachi S-4300SE/N SEM instrument. Testing specimens were cryofractured in liquid nitrogen and their outer surfaces were covered with a thin gold film to avoid charging of electrons. The SEM machine was operated at an accelerating voltage of 20 kV.

Thermal stability and related properties of the membranes were assessed by thermogravimetric analysis using a TGA/SDTA 851 (Mettler Toledo) system in air by heating from ambient temperature to 700 °C at a heating rate of 10 °C min^{-1}.

CO_2 and N_2 adsorption isotherms evaluated at 77 and 298 K using a Quantachrome Autosorb iQ gas sorption analyzer helped to assess various microporous characteristics (e.g., specific BET and Langmuir surface areas, total microporous volume, CO_2 and N_2 gas uptakes) of the membranes. The membrane samples were chopped into tiny pieces and degassed at 100 °C under vacuum ($<10^{-6}$ bar) for 5 hours. Physisorption data of CO_2 and N_2 gases were measured at 298 K under a gas pressure ranging from 10^{-6} to 1 bar.

Gas Permeation Measurements

Pure gas (CO_2 and N_2) transport properties (i.e., permeability, ideal selectivity, and separation performance) of the MMMs were assessed using a single gas permeation cell following the variable pressure (constant volume) method at a temperature of 298 K (Yu *et al.*, 2010). After measuring its average thickness the membrane was fixed in the permeation cell. While keeping the feed side valve closed, both the upstream (feed side) and downstream (permeate side) lines of the cell were evacuated. The valve between the permeate side line and the vacuum pump was then closed followed by opening the feed side valve to maintain a low feed pressure (e.g., 0.1 bars) for a specific time (i.e., 2 h) to record the permeation measurements. The feed pressure was then intermittently increased and data were collected after at least 1 h of stabilization for each interval. At least three replicas were prepared and tested corresponding to each composition of the MMMs in order

to assess error and identify imperfect membranes.

Gas permeability (P_i, *Barrer*) of the membrane was computed using eq. (2):

$$P_i = \frac{22414}{A} \times \frac{V}{RT} \times \frac{l}{\Delta P_i} \frac{dP_i}{dt} \quad (2)$$

where *l, A, V, R, T,* ΔP and $\Delta P_i/dt$ are respectively membrane thickness (*cm*), membrane active area (cm^2), downstream volume (cm^3), universal gas constant (6236.56 cm^3 *cmHg/mol/K*), absolute temperature (*K*), pressure difference across the membrane (*psi*), and permeation rate (*psi/s*) of component i.

Time-lag method, suggested by Paul and Kemp (1973), was used to determine the diffusion coefficient (D) by using the *diffusivity vs. time-lag* (D-θ) relationship for MMMs:

$$D = \frac{l^2}{6\theta}\left[1 + \frac{6K}{y^3}\left\{\frac{y^2}{2} + y - (1+y)\ \ln(1+y)\right\}\left(\frac{V_d}{V_p}\right)\right] \quad (3)$$

where V_d and V_p are respectively the volume fractions of filler and polymer phases; K and y are adsorption parameters determined from a Langmuir adsorption isotherm.

The solubility coefficient (S) can be calculated from Eq. (4):

$$S = \frac{P}{D} \quad (4)$$

The ideal selectivity of gas i over j (α_{ij}) can be determined using Eq. (5):

$$\alpha_{ij} = \frac{P_i}{P_j} = \left(\frac{D_i}{D_j}\right)\left(\frac{S_i}{S_j}\right) \quad (5)$$

where (D_i/Dj) and (S_i/S_j) represent diffusion- and solubility-based selectivity terms, respectively.

RESULTS AND DISCUSSION

The experimentally obtained results of different characterization techniques i.e., XRD, SEM, TGA, gas sorption and gas permeation are briefly described here.

Powder X-ray Diffraction

Powder X-ray diffraction is an effective exercise to analyze the effect of nanofillers on the configuration of polymer chains in MMMs and to validate the existence of crystalline materials in amorphous polymer matrices. XRD measurements in the range of 2-50° were registered to ensure the existence of CNTs and ZIF-301 crystalline structure in hybrid membranes as shown in Fig. 1. The specific peak intensities emerging at 2θ positions of 5.7°, 6.8° and 11.6° in XRD patterns of MMMs correspond to ZIF-301 nanocrystals [28], while those appearing at 25.8° and 44.1° confirmed the dispersion of CNTs within the PSF matrix (Gupta *et al.*, 2013).

The good coincidence of XRD patterns of MMMs with those of CNTs and ZIF-301 nanocrystals suggests their crystalline preservation after doping into polymer matrix. Furthermore, the peak intensifications at the specified 2θ positions are proportional to the loading levels of respective nanofillers incorporated in the composite membranes. All the membranes displayed a characteristic broad peak of PSF centered at an angle of 2θ = 17.2°. In addition, the slight shift of the broad peak position (2θ) of bare PSF from 17.2° (d-spacing = 5.21 Å) to 17.4° (d-spacing = 5.14 Å) can be attributed to the strong filler-polymer interactions, thus reducing the polymer inter-chain distance. The inter-chain size reduction facilitates CO_2/N_2 selectivity due to size exclusion phenomenon.

Morphology of PSF/CNTs/ZIF-301 MMMs

The morphology and structural characteristics of the hybrid membranes mainly depend upon the nature of the organic polymer matrix and included inorganic filler(s). Cross sectional micrographs of MMMs were probed by SEM in order to investigate the morphology of the prepared MMMs, the adhesion between filler-polymer interface and the dispersion of CNTs and ZIF-301 nanoparticles within the polymer matrix as illustrated in Fig. 2. All MMMs filled with varying loadings of nanofillers exhibited continuous phases, almost free of interfacial voids. In case of composite membranes containing high loadings of CNTs (ca. 8 and 10 wt %) and low ZIF-301 contents (i.e., 6 and 12 wt %), the CNTs agglomerated owing to their large surface energy while ZIF-301 nanocrystals showed homogeneous dispersion and good polymer-filler adhesion on account of their tiny particle size (Figs. 2 [B] and [C]). The MMMs filled with high ZIF-301 (e.g. 24 and 30 wt %) and low CNTs (i.e., 2 and 4 wt %) loadings (Figs. 2 [E] and [F]) demonstrated relatively uniform CNTs distribution due to reduced total surface energy of CNTs, but indications of slight aggregation of ZIF-301 nanoparticles with PSF matrix are observed owing to relatively reduced adhesion between ZIF-301 nanocrystals and the PSF matrix. The mixed-matrix membrane containing optimal loading of nanofillers (6 wt % CNTs and 18 wt % ZIF-301) demonstrated uniform dispersion and good filler-polymer interfacial adhesion as the cross-sectional view of MMM exhibits a defect-free interconnected network morphology (Fig. 2 [D]). The controlled morphology of ZIF-301 nanocrystals dispersed in the optimized MMM provided a significant steric effect to reduce CNTs aggregation; conversely, the strong polymer-filler interaction led to homogeneous dispersion of ZIF-301 nanocrystals. The synergistic effect of ZIF-301 nanocrystals and CNTs

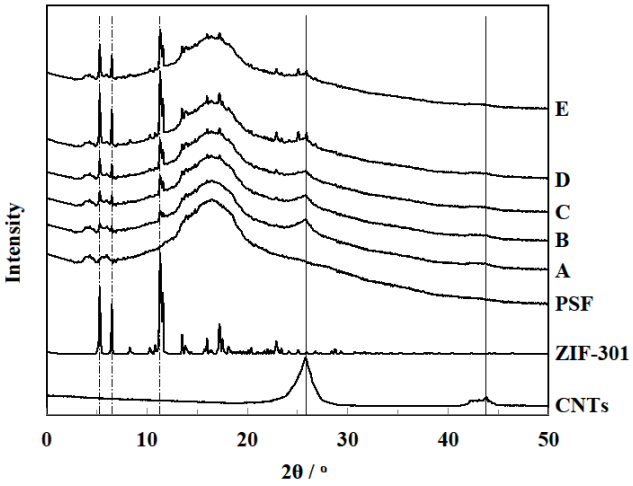

Figure 1. Powder X-ray patterns of CNTs, ZIF-301, bare PSF, PSF/CNTs(10)/ZIF-301(6) [A], PSF/CNTs(8)/ZIF-301(12) [B], PSF/CNTs(6)/ZIF-301(18) [C], PSF/CNTs(4)/ZIF-301(24) [D], and PSF/CNTs(2)/ZIF-301(30) [E] MMMs containing different loadings of CNTs and ZIF-301 nanocrystals.

helped to orient some of the CNTs parallel to the thickness of membranes to offer relatively shorter gas permeation passages within the membrane.

Thermal Gravimetric Analysis

To assess the mutual effect of CNTs and ZIF-301 nanofillers on phase transitions, thermal stability, chemical and physical behavior of MMMs, TGA-DTG analyses of bare PSF and hybrid membranes were performed in the range of 100-700 °C. The TGA curves of the prepared membranes showed consistent decomposition profiles demonstrating a two-stage weight loss owing to desolvation (at around 100-180 °C) and pyrolysis (460-660 °C) processes as indicated in Fig. 3 [A]. The desolvation step refers to the release of volatile solvent molecules such as DMF, water, CCl_4 etc. confined within the pores of MMMs, while the decomposition of organic ligands of the imidazole frameworks and the degradation of CNTs and PSF constituting entities occur during pyrolysis step. For all MMM samples, ZIF-301 particles, CNTs and PSF are completely burnt at the end of the thermal characterization, leaving metallic zinc behind as ash. The increase in residual mass of MMMs with increasing ZIF-301 contents is mainly due to the increased metallic zinc present in ZIF-301. The residual ash left behind at the end of the thermal test validated the nominal mass contents of nanofillers incorporated in the corresponding MMMs.

The thermal stability of a material can be evaluated, via TGA analysis, in terms of $T_{d5\%}$ *and* $T_{d10\%}$ values- the temperatures at which the test specimen loses 5 and 10 percent of its weight, respectively (Xiao *et al.*, 2007). Being an increasing function of nanofiller contents, values of $T_{d5\%}$ and $T_{d10\%}$ occur in the range of 177-188 °C and 591-599 °C, respectively. Some of the notable thermal properties of hybrid membranes are outlined in Table 1. The derivative thermogravimetric (DTG)

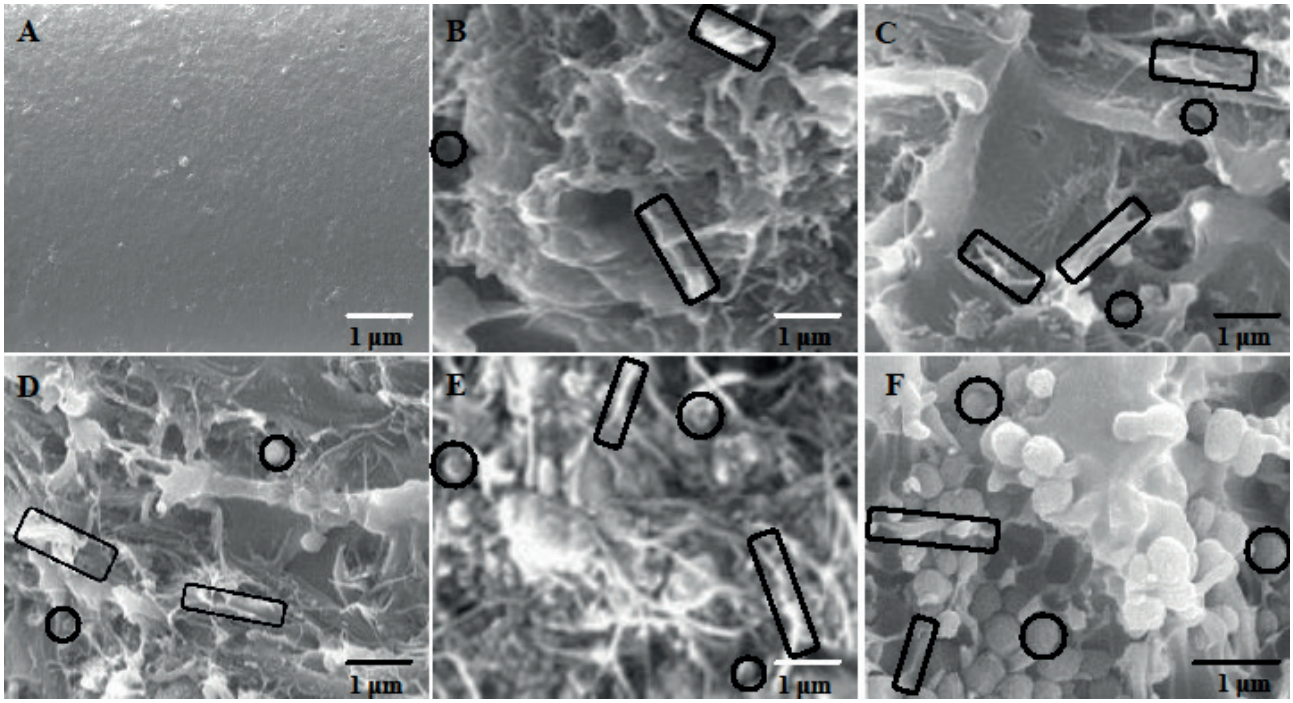

Figure 2. Scanning electron micrographs of bare PSF [A], PSF/CNTs(10)/ZIF-301(6) [B], PSF/CNTs(8)/ZIF-301(12) [C], PSF/CNTs(6)/ZIF-301(18) [D], PSF/CNTs(4)/ZIF-301(24) [E], and PSF/CNTs(2)/ZIF-301(30) [F] MMMs containing different loadings of CNTs (enclosed by rectangles) and ZIF-301 nanocrystals (surrounded by circles).

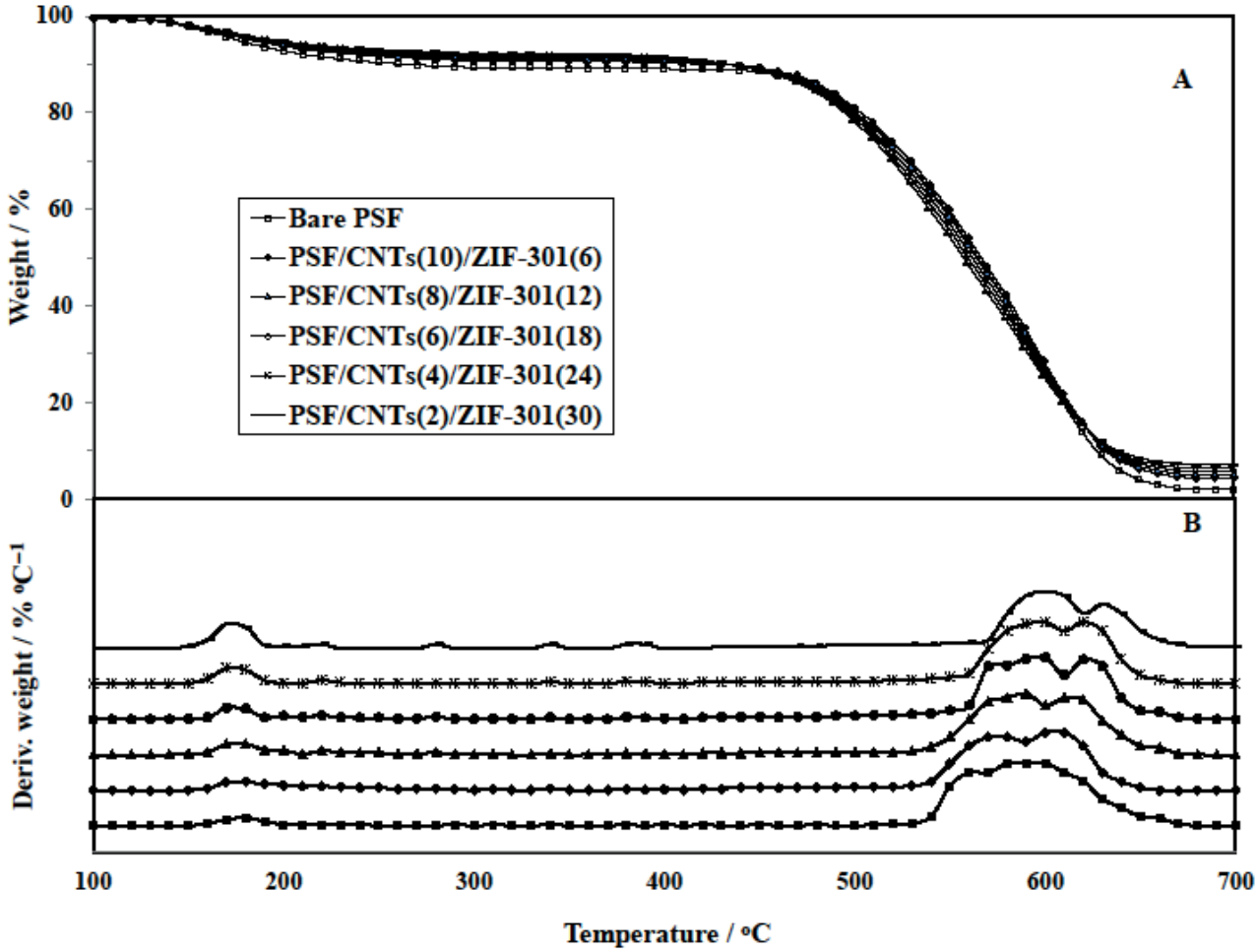

Figure 3. TGA-DTG curves: TGA [A] and DTG [B] of bare PSF and MMMs containing different loadings of CNTs and ZIF-301 nanocrystals.

curves illustrated in Fig. 3 [B] provide essential data on pyrolysis rates in terms of the 1st and 2nd DTG peaks. The degree of rigidity of the polymer chains in MMMs can be determined in terms of glass transition temperature (T_g), 1st and 2nd DTG peak values. The upgrading of these parameters, especially T_g, with increased nanofiller loadings (Table 1), signifies improved rigidity of MMMs due to the constrained motion of polymer chains resulting from mutual interactions among polymer chains and nanofiller entities.

In contrast to a bare PSF membrane, occurrence of thermal disintegration of hybrid membranes at higher temperatures can be attributed to improved polymer-filler interactions and good thermal stability of CNTs and ZIF-301 nanocrystals. Thermal stability of mixed membranes, determined in terms of T_g, improved with increasing nanofiller loadings as supported by weight loss curves. Since the maximum temperature observed in different gas separation and combustion processes occurs in the range of 30 to 350 °C, these MMMs can safely be used in gas separation applications (Chang *et al.*, 2003).

Gas Sorption Analysis

N_2 adsorption isotherms, normally performed at 77 K under relative pressure of 0.3 bar, were applied to measure surface area and microporosity of the membranes. CO_2 and N_2 adsorption isotherms were obtained to determine their respective loading capacities under low pressure at 298 K as shown in Fig. 4.

Key physical macroscopic properties (density, fractional volume of nanofillers) and some other important microporous characteristics such as Brunauer-Emmett-Teller (S_{BET}) and Langmuir (S_{Lang}) surface areas, total micropore volume, CO_2 and N_2 uptakes, and CO_2/N_2 adsorption selectivity of the specimen were improved with the incorporation of nanofillers as summarized in Table 2. These outcomes significantly corroborated the existence of uniform distribution, improved interfacial adhesion between PSF matrix and nanofillers resulting in good quality MMMs.

As compared to bare PSF, CO_2 uptake for all the MMMs considerably improved with increasing pressure on account of specific chemical affinity of both the nanofillers for quadrupolar CO_2 molecules. The hybrid membrane

Table 1. Characteristic temperatures of membrane materials acquired from TGA-DTG data

Sample Designation	T_g (°C)	$T_{d5\%}$ (°C)	$T_{d10\%}$ (°C)	1st DTG peak (°C)	2nd DTG peak (°C)	Residual mass (%)
Bare PSF	177	177	261	177	591	2.1
PSF/CNTs(10)/ZIF-301(6)	181	180	430	180	594	4.4
PSF/CNTs(8)/ZIF-301(12)	182	183	432	182	595	4.9
PSF/CNTs(6)/ZIF-301(18)	185	188	434	184	596	5.7
PSF/CNTs(4)/ZIF-301(24)	187	192	435	186	597	6.4
PSF/CNTs(2)/ZIF-301(30)	189	196	436	188	599	7.1

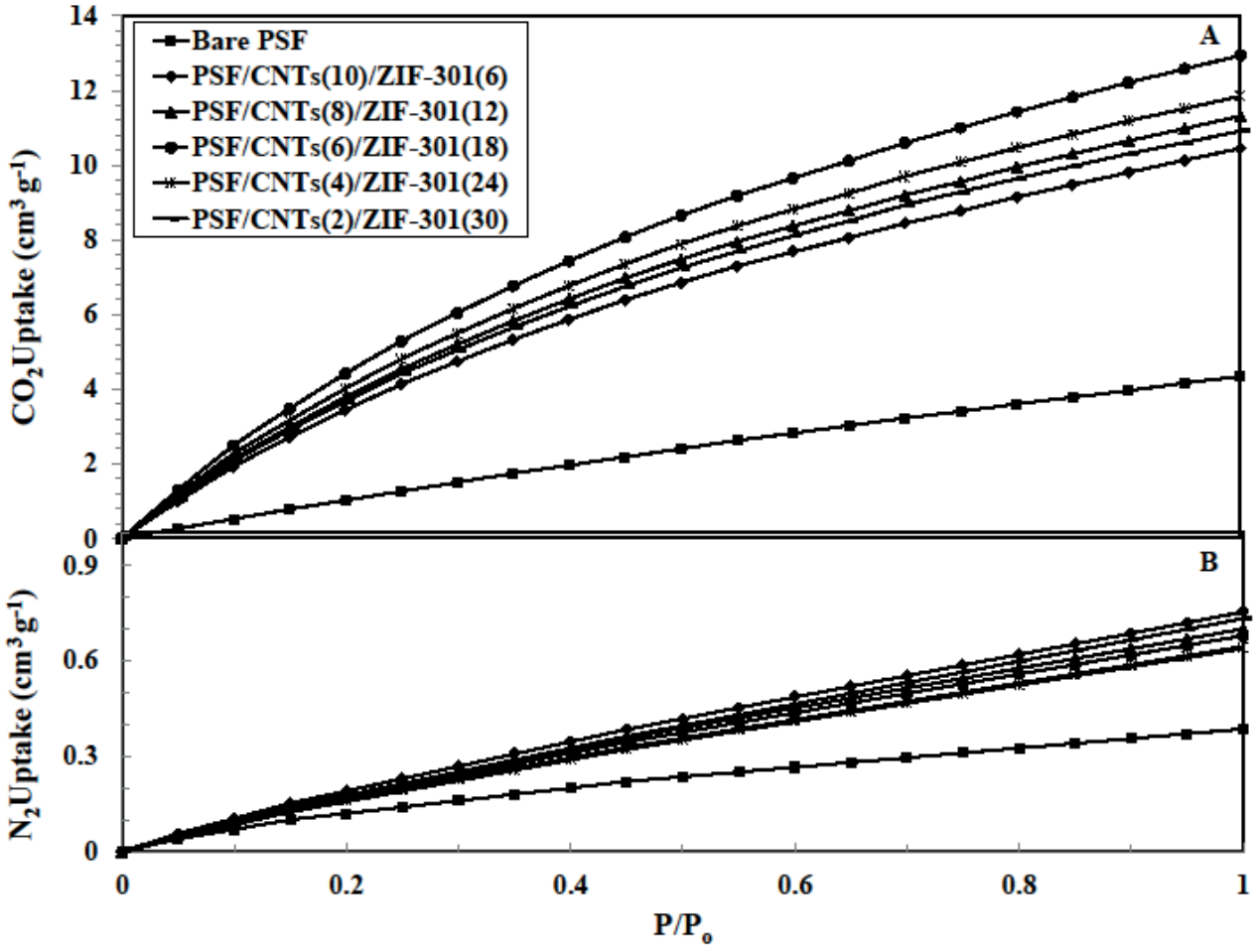

Figure 4. CO_2 [A] and N_2 [B] adsorption isotherms for bare PSF and PSF/CNTs/ZIF-301 MMMs containing varying loadings of CNTs and ZIF-301 nanocrystals at 298 K.

filled with 6 wt % CNTs and 18 wt % ZIF-301 nanocrystals yielded the highest CO_2 loading, ca. 14 cm^3/g (≈ 0.7 mmol/g) at 298 K. The N_2 gas was almost linearly adsorbed with pressure up to 1 bar for all the membranes, indicating very poor chemical affinity for nanofillers. In addition, all the membranes showed preferably high adsorption affinity for CO_2 as compared to N_2, especially at low CO_2 partial pressure. The CO_2/N_2 sorption selectivities of the MMMs significantly increased with nanofiller (especially ZIF-301) loadings. These findings suggest the fabricated MMMs as potential candidates to separate a CO_2 from CO_2/N_2 mixture from post combustion flue gas.

Gas Permeation Properties

Single gas CO_2 and N_2 permeation experiments were performed to evaluate the permeability and ideal selectivity of the prepared membranes under dry and wet conditions

Table 2. Physical and microporous properties of bare PSF and PSF/CNTs/ZIF-301 MMMs

Sample Designation	Density ($g\ cm^{-3}$)	Φ_d (%)	S_{BET} (m^2g^{-1})	S_{Lang} (m^2g^{-1})	V_{micro} (m^3g^{-1})	CO_2 uptake (cm^3g^{-1})	N_2 uptake (cm^3g^{-1})	$\acute{a}_{CO_2/N_2}$
Bare PSF	1.25	0.00	12	18	0.02	4.3	0.39	11
PSF/CNTs(10)/ZIF-301(6)	1.347	12.41	130	170	0.23	9.1	0.63	14
PSF/CNTs(8)/ZIF-301(12)	1.342	17.24	160	190	0.27	11.3	0.76	15
PSF/CNTs(6)/ZIF-301(18)	1.337	21.99	180	220	0.32	13.7	0.91	15
PSF/CNTs(4)/ZIF-301(24)	1.332	26.67	200	250	0.28	11.8	1.1	11
PSF/CNTs(2)/ZIF-301(30)	1.327	31.28	230	280	0.23	10.3	1.2	9

at 25 °C subjected to an upstream pressure of 2 bar. On account of favorable CO_2-nanofillers mutual affinity, CO_2 permeability and CO_2/N_2 ideal selectivity of the hybrid membranes were significantly improved by adding CNTs and ZIF-301 nanocrystals, as depicted in Figs. 5 and 8, respectively. The permeation experiments performed under wet conditions led to a slight improvement of CO_2 transport properties along with its separation from N_2.

Due to their relatively large pore diameter and smooth inner surfaces, the exclusive incorporation of CNTs into the polymer matrix extensively improved CO_2 permeability, but at the expense of deteriorated CO_2/N_2 permselectivity (Li *et al.*, 2015). The sole inclusion of ZIF-301 nanocrystals into polymer-based hybrid membranes reasonably increased both CO_2 permeability and CO_2/N_2 permselectivity due to the chemical structure of ZIF-301. Both the CO_2 permeability and CO_2/N_2 ideal selectivity of the hybrid membranes were appreciably enhanced by the synergistic effect of adding CNTs and ZIF-301 nanofillers. The most favorable optimal filler loading was found to be 6 wt % CNTs and 18 wt % ZIF-301 nanocrystals since it exhibits the maximum CO_2 permeability and maximum CO_2/N_2 ideal selectivity among all the prepared MMM samples. At the optimal filler loading the CO_2 permeability of the MMM was determined to be 19 Barrer with CO_2/N_2 selectivity of 48. The most preferable loading favored homogeneous distribution of the nanofillers so as to exploit the pathways of CNTs pores to amplify CO_2 permeability and the CO_2/N_2 selective affinity of amine-functionalized ZIF-301 nanocrystals to render high selectivity.

The gas permeation through a membrane occurs via solubility followed by diffusivity of the permeating gas molecules; this phenomenon can be well elucidated by estimating the coefficient of solubility (S) and coefficient of diffusivity (D) of CO_2 and N_2 gas molecules in mixed-matrix membranes. The essential data pertaining to gas diffusivity and solubility for the prepared membranes are illustrated in Figs. 6 and 7, respectively.

The diffusivity coefficients of both CO_2 and N_2 were slightly changed with different nanofiller loadings reaching a maximum value at the optimal nanofiller loading. The diffusivities were improved due to the preferential orientation and close packing of cylindrical smooth-walled CNTs within the polymer matrix. The variation in CO_2 solubility coefficient was much pronounced as compared to that of N_2; the solubility coefficient of CO_2, in contrast to N_2, was significantly improved at the optimum loading. The solubility coefficient, in general, depends on both chemical composition and structural arrangement of the membrane. The basic nature of both CNTs hydroxyl groups and ZIF-301 amine groups generated a synergistic effect to preferably adsorb the acidic CO_2 molecules as compared to non-polar N_2 molecules. This effect resulted in higher CO_2 solubility and limited that of N_2, consequently improving the CO_2/N_2 solubility-based selectivity. The improved permselectivity of CO_2 over N_2 can also be ascribed to the enlarged number of interaction sites and basic functional groups due to the addition of CNTs and ZIF-301 nanocrystals into the PSF matrix.

The time-lag method (eq. 6) was used to determine the values of diffusion coefficients. CO_2 and N_2 adsorption

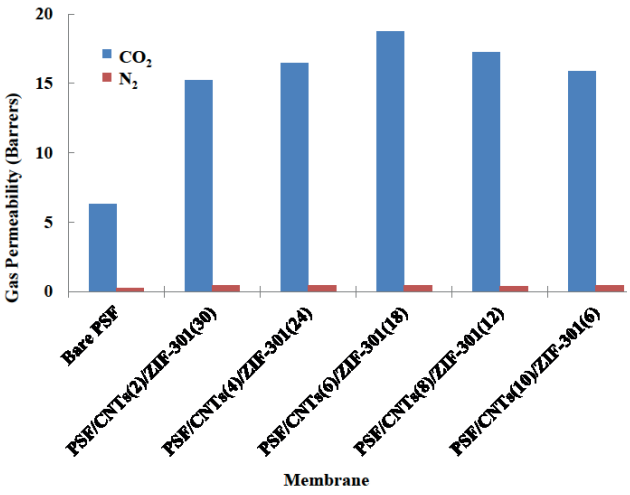

Figure 5. CO_2 and N_2 permeability of bare PSF, PSF/CNTs(10)/ZIF-301(6), PSF/CNTs(8)/ZIF-301(12), PSF/CNTs(6)/ZIF-301(18), PSF/CNTs(4)/ZIF-301(24), and PSF/CNTs(2)/ZIF-301(30) MMMs containing different loadings of CNTs and ZIF-301 nanocrystals.

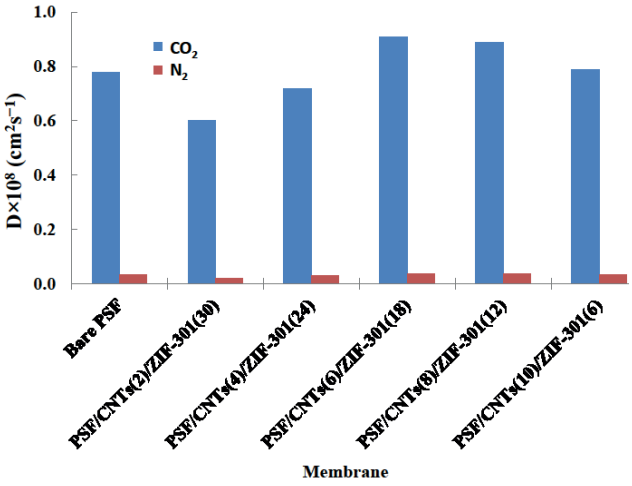

Figure 6. Pure gas coefficients of diffusion (D) for bare PSF, PSF/CNTs(10)/ZIF-301(6), PSF/CNTs(8)/ZIF-301(12), PSF/CNTs(6)/ZIF-301(18), PSF/CNTs(4)/ZIF-301(24), and PSF/CNTs(2)/ZIF-301(30) MMMs containing different loadings of CNTs and ZIF-301 nanocrystals.

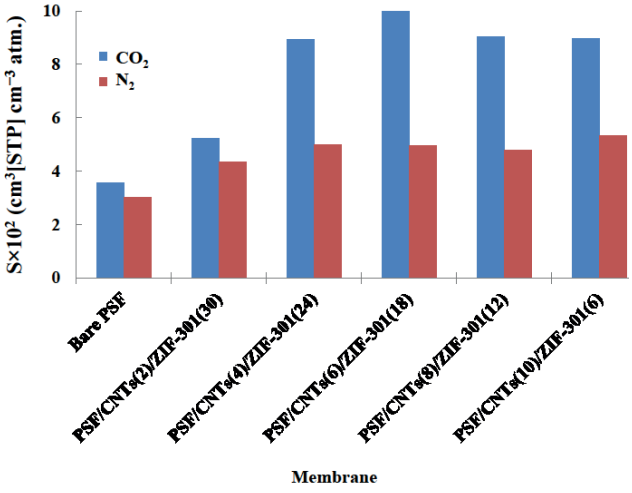

Figure 7. Pure gas coefficients of solubility (S) for bare PSF, PSF/CNTs(10)/ZIF-301(6), PSF/CNTs(8)/ZIF-301(12), PSF/CNTs(6)/ZIF-301(18), PSF/CNTs(4)/ZIF-301(24), and PSF/CNTs(2)/ZIF-301(30) MMMs containing different loadings of CNTs and ZIF-301 nanocrystals.

isotherms obtained at 25 °C under varying pressure helped to calculate Langmuir parameters to determine the correction parameters (bracketed term in eq. 3). The D values thus determined were used to calculate solubility coefficients of the membranes under the same conditions of temperature and pressure using eq. 4. The values of gas diffusivity coefficient selectivity (D_{CO2}/D_{N2}) slightly varied with different nanofiller loadings, while the gas solubility coefficient selectivity (S_{CO2}/S_{N2}) significantly changed for all the hybrid membranes attaining a peak value for the optimized MMM containing 6 wt % CNTs and 18 wt % ZIF-301 as shown in Fig. 8.

Almost defect-free CNTs permitted both CO_2 and N_2 gas molecules to diffuse quickly through its internally smooth-walled channels. Since the proper distribution of CNTs in the PSF matrix acted as efficient pathways to proficiently transport gas molecules, the overall gas permeability was highly improved. Also the preferential solubility of CO_2, over N_2, in the ZIF-301 nanocrystals significantly improved its permeation through the hybrid membranes. The narrowing down of pore size of MMMs due to incorporation of ZIF-301 nanocrystals may limit the N_2 adsorption as compared to CO_2. In a nutshell, the CO_2/N_2 permselectivities of composite membranes are improved due to selective CO_2 solubility and restricted N_2 diffusion. Both the nanofillers mutually interacted so as to offer controlled passages for improved CO_2 permeability and CO_2/N_2 selectivity through the composite membranes. The overall analysis based on improved performance of PSF/CNTs/ZIF-301 MMMs strongly supports the development of a true mixed matrix membrane.

A comparison of the CO_2/N_2 gas pair separation performance of nanofilled MMMs, along with Robeson 1991 and 2008 upper bounds (Robeson, 2008), is made on a permeability-selectivity chart as illustrated in Fig. 9. The diagram indicates that the incorporation of CNTs and ZIF-301 nanofillers into the PSF matrix enhanced the permselectivity of the MMMs as compared to a bare polysulfone membrane. The permselectivity values of all the composite membranes reported here are located between the 1991- and 2008-upper bound lines, an important achievement of this work.

Since a membrane having high CO_2 permeability coupled with improved CO_2/N_2 ideal selectivity characteristics fulfills industrial requirements, it corroborates that CNTs and ZIF-301 nanofillers are competent materials to fabricate MMMs for post combustion carbon capture.

CONCLUSIONS

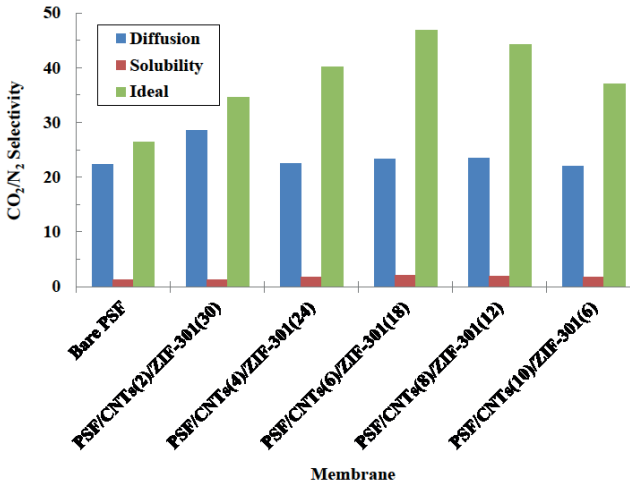

Figure 8. CO_2/N_2 selectivity values (based on diffusion, solubility and ideal case) of bare PSF, PSF/CNTs(10)/ZIF-301(6), PSF/CNTs(8)/ZIF-301(12), PSF/CNTs(6)/ZIF-301(18), PSF/CNTs(4)/ZIF-301(24), and PSF/CNTs(2)/ZIF-301(30) MMMs containing different loadings of CNTs and ZIF-301 nanocrystals.

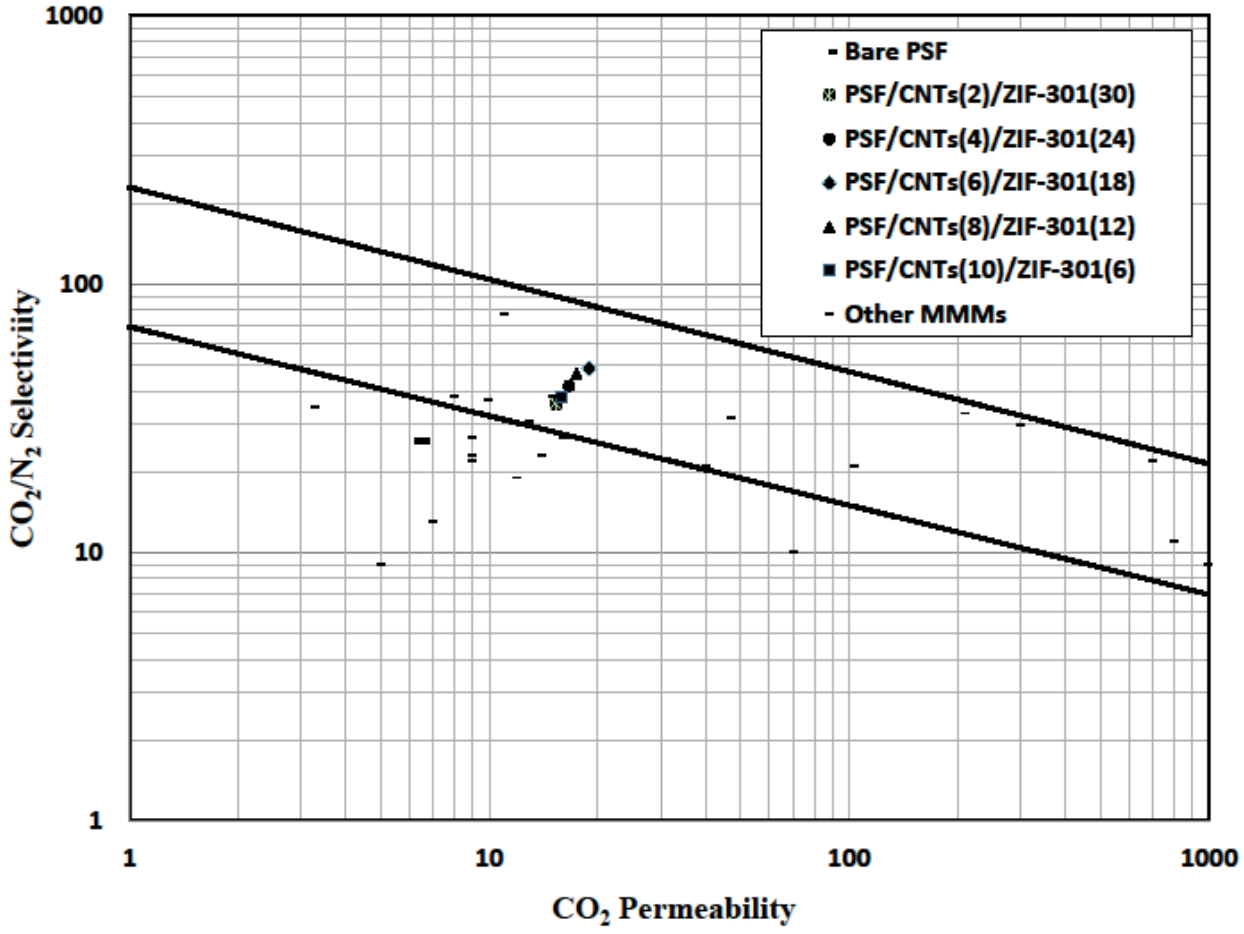

Figure 9. Comparison of CO_2/N_2 separation performance of PSF/CNTs/ZIF-301 MMMs with other MOF containing MMMs obtained from literature data. The Robeson 1991- and 2008- upper bounds for polymer separation performance are also shown.

Hydrothermally stable high performance mixed-matrix membranes were fabricated by incorporating multi-walled CNTs and ZIF-301 nanofillers to selectively capture CO_2 from post combustion flue gas. Characterization of the MMMs carried out by XRD, TGA, SEM and gas sorption experiments indicated that they are thermally stable, microporous, partially crystalline materials exhibiting homogeneous nanofillers dispersion and good interfacial matrix-filler adhesion without adding any compatibilizing agent. The hybrid membranes prepared in this work demonstrated a more than 5-fold increment in CO_2 permeability as compared to that of a bare PSF membrane, while the CO_2/N_2 ideal selectivity was enhanced by more than 3-fold. Furthermore, the MMMs perform well under wet conditions as compared to dry ones. The separation performance of the composite membranes produced in this work were above the Robeson 1991 upper bound and the CO_2/N_2 ideal selectivity is considered to be high enough to meet industrial applications.

ACKNOWLEDGEMENT

The authors are thankful to KACST-TIC on Carbon Capture and Sequestration (CCS), King Fahd University of Petroleum and Minerals, Dhahran, Kingdom of Saudi Arabia for providing support for this work.

ABBREVIATIONS

Symbols

A effective membrane area (cm^2)
Å Angstrom
D diffusion coefficient (cm^2/s)
K adsorption parameter determined from Langmuir adsorption isotherm
L membrane thickness (cm)
m mass or weight of the specimen
P gas permeability (Barrer; 1 Barrer = 10^{-10} cm^3 (STP) cm/(cm s cmHg))
R universal gas constant (6236.56 cm^3 cmHg/mol/K)

S solubility coefficient (cm^3 (STP)/cm^3 cmHg)
T absolute temperature (K)
V cell downstream volume (cm^3)
y parameter to be determined from Langmuir adsorption isotherm
Δp pressure difference across the membrane (psi)
ΔP/dt gas permeation rate (psi/s) in terms of time rate of pressure

Greek letters

α membrane gas selectivity
θ X-ray diffraction angle (°)
ρ bulk density (g/cm^3)
Φ fractional volume of fillers (%)

Subscripts

C continuous phase
D dispersed phase
d5% 5 percent specimen weight loss
d10% 10 percent specimen weight loss
eff effective
g glass transition
i gas 'i'
j gas 'j'
m polymer matrix

Superscripts

o degree

REFERENCES

Ahn, J., Chung, W.-J., Pinnau, I. and Guiver, M.D., Polysulfone/silica nanoparticle mixed-matrix membranes for gas separation. J. Membr. Sci., 314, 123-133 (2008).

Baker, R.W., Future directions of membrane gas separation technology. J. Ind. Eng. Chem. Res., 41 1393–1411 (2002).

Chamberlain, T.W., Meyer, J.C., Biskupek, J., Leschner, J., Santana, A., Besley, N.A., Bichoutskaia, E., Kaiser, U. and Khlobystov, A.N., Reactions of the inner surface of carbon nanotubes and nanoprotrusion processes imaged at the atomic scale. Nat. Chem., 3, 732–737 (2011).

Chang, A.C.C., Chuang, S.S.C., Gray, M. and Soong, Y., In-situ infrared study of CO_2 adsorption on SBA-15 grafted with γ-(aminopropyl) triethoxysilane. Energy Fuels, 17, 468-473 (2003).

Chen, H. and Sholl, D.S., Predictions of selectivity and flux for CH_4/H_2 separations using single walled carbon nanotubes as membranes. J. Membr. Sci., 269, 152–160 (2006).

Chen Zhang, Kuang Zhang, Liren Xu, Ying Labreche, Brian Kraftschik and Koros, W.J., Highly scalable ZIF-based mixed-matrix hollow fiber membranes for advanced hydrocarbon separations. AIChE J., 60, 2625–2635 (2014).

Cong, H.L., Zhang, J.M., Radosz, M. and Shen, Y.Q., Carbon nanotube composite membranes of brominated poly(2,6-diphenyl-1,4-phenylene oxide) for gas separation. J. Membr. Sci., 294, 178–185 (2007).

D'Alessandro, D. M., Smit, B. and Long, J. R., Carbon Dioxide Capture: Prospects for New Materials. Angew. Chem. Int. Ed., 49, 6058-6082 (2010).

Fawas, E.P., Kapantaidakis, G.C., Nolan, J.W., Mitropoulos, A.C. and Kanellopoulos, N.K., Preparation, characterization and gas permeation properties of carbon hollow fiber membranes based on Matrimid® 5218 precursor. J. Mater. Process. Technol., 186, 102–110 (2007).

Galve, A., Sieffert, D., Staudt, C., Ferrando, M., Güell, C., Téllez, C. and Coronas, J., Combination of ordered mesoporous silica MCM-41 and layered titanosilicate JDF-L1 fillers for 6FDA-based copolyimide mixed matrix membranes. J. Membr. Sci., 431, 163-170 (2013).

Ge, L., Wang, L., Rudolph, V. and Zhu, Z., Hierarchically structured metal-organic framework/vertically-aligned carbon nanotubes hybrids for CO_2 capture. RSC Adv., 3, 25360-25366 (2013).

Gin, D.L. and Noble, R.D., Designing the next generation of chemical separation membranes. Science, 332, 674-676 (2011).

Gorgojo, P., Uriel, S., Tellez, C. and Coronas, J., Development of mixed matrix membranes based on zeolite Nu-6(2) for gas separation. J. Microporous Mesoporous Mater., 115, 85–92 (2008).

Gupta, V. and Saleh, T., Synthesis of Carbon Nanotube-Metal Oxides Composites; Adsorption and Photo-Degradation. Carbon, 59, 308–314 (2013).

Harold, B., Jeazet, T., Staudt, C. and Janiak, C., Metal-organic frameworks in mixed-matrix membranes for gas separation. Dalton Trans., 41, 14003–14027 (2012).

Herzog, H. and Golomb, D., Carbon capture and storage from fossil fuel use. Encyc. Energy, 1, 277-287 (2004).

Hussain, A. and Hägg, M.B., A feasibility study of CO_2 capture from flue gas by a facilitated transport membrane. J. Membr. Sci., 359, 140-148 (2010).

Ismail, A.F., Goh, P.S., Sanip, S.M. and Aziz, M., Transport and separation properties of carbon nanotube-mixed matrix membrane. Sep. Purif. Technol., 70, 12–26 (2009).

Jacobson, M. Z., Review of Solutions to Global Warming, Air Pollution, and Energy Security. Energy Environ. Sci., 2, 148-173 (2009).

Kim, S., Marand, E., Ida, J. and Guliants, V.V., Polysulfone and mesoporous molecular sieve MCM-48 mixed matrix membranes for gas separation. Chem. Mater., 18, 1149-1155 (2006).

Kim, S. and Marand, E., High permeability nanocomposite membranes based on mesoporous MCM-41 nanoparticles in a polysulfone matrix. Microp. Mesop. Mater., 114, 129-136 (2008).

Kim, S., Chen, L., Johnson, J.K. and Marand, E., Polysulfone and functionalized carbon nanotube mixed matrix membranes for gas separation: Theory and experiment. J. Membr. Sci., 294, 147–158 (2007).

Kim, S., Jinschek, J.R., Chen, H., Sholl, D.S. and Marand, E., Scalable fabrication of carbon nanotube/polymer nanocomposite membranes for high flux gas transport. Nano Lett., 7, 2806–2811 (2007).

Li, T., Pan, Y., Peinemann, K.V. and Lai, Z., Carbon dioxide selective mixed matrix composite membrane containing ZIF-7 nano-fillers. J. Membr. Sci., 425-426, 235-242 (2013).

Li, X., Ma, L., Zhang, H., Wang, S., Jiang, Z., Guo, R., Wu, H., Cao, X.Z., Yang, J. and Wang, B., Synergistic effect of combining carbon nanotubes and graphene oxide in mixed matrix membranes for efficient CO_2 separation. J. Memb. Sc., 479, 1-10 (2015).

Liu, Y., Peng, D., He, G., Wang, S., Li, Y., Wu, H. and Jiang, Z., Enhanced CO_2 permeability of membranes by incorporating polyzwitterion@CNT composite particles into polyimide matrix. ACS Appl. Mater. Interfaces, 6, 13051-13060 (2014).

MacDowell, N., Florin, N., Buchard, A., Hallett, J., Galindo, A., Jackson, G., Adjiman, C. S., Williams, C. K., Shah, N. and Fennell, P., An Overview of CO_2 Capture Technologies. Energy Environ. Sci., 3, 1645-1669 (2010).

Mahajan, R. and Koros, W.J., Factors controlling successful formation of mixed-matrix gas separation materials. Ind. Eng. Chem. Res., 39, 2692–2696 (2000).

Merkel, T.C., Freeman, B.D., Spontak, R.J., He, Z., Pinnau, I., Meakin, P. and Hill, A. J., Ultrapermeable, reverse-selective nanocomposite membranes. Science, 296, 519-522 (2002).

Mohammad Askari and Chung, T.S., Natural gas purification and olefin/paraffin separation using thermal crosslink ableco-polyimide/ZIF-8 mixed matrix membranes. J. Membr. Sci., 444, 173–183 (2013).

Nhung, T.T.N., Furukawa, H., Gandara, F., Nguyen, H.T., Cordova, K.E. and Yaghi, O.M., Selective capture of carbon dioxide under humid conditions by hydrophobic chabazite-type zeolitic imidazolate frameworks. Angew. Chem., 126, 10821–10824 (2014).

Pandey, P. and Chauhan, R.S., Membranes for gas separation. Prog. Polym. Sci., 26, 853-893 (2001).

Paul, D.R. and Kemp, D.R., The diffusion time lag in polymer membranes containing adsorptive fillers. J. Polym Sc: Polym. Symp., 41, 79–93 (1973).

Reid, B.D., Ruiz-Trevino, A., Musselman, I.H., Balkus, K.J. and Ferraris, J.P., Gas permeability properties of polysulfone membranes containing the mesoporous molecular sieve MCM-41. Chem. Mater., 13, 2366-2373 (2001).

Robeson, L. M., The upper bound revisited. J. Membr. Sc., 320, 390-400 (2008).

Sholl, D.S. and Johnson, J.K. Making high-flux membranes with carbon nanotubes. Science, 312, 1003-1004 (2006).

Staudt-Bickel, C. and Koros, W.J., Improvement of CO_2/CH_4 separation characteristics of polyimides by chemical crosslinking. J. Membr. Sci., 155, 145-154 (1999).

Skoulidas, A.I., Sholl, D.S. and Johnson, J.K., Adsorption and diffusion of carbon dioxide and nitrogen through single-walled carbon nanotube membranes. J. Chem. Phys., 124, 054708 (2006).

Song, Q. et al. Zeolitic imidazolate framework (ZIF-8) based polymer nanocomposite membranes for gas separation. Energy Environ. Sci., 5, 8359-8369 (2012).

Valero, M., Zornoza, B., Téllez, C. and Coronas, J., Mixed matrix membranes for gas separation by combination of silica MCM-41 and MOF NH2-MIL-53 (Al) in glassy polymers. Microporous Mesoporous Mater., 192, 23-28 (2013).

Vu, D.Q., Koros, W.J. and Miller, S.J., Mixed matrix membranes using carbon molecular sieves. II. Modeling permeation behavior. J. Membr. Sci., 211, 335-348 (2003).

Xiao, Y. and Chung, T.-S., Grafting thermally labile molecules on cross-linkable polyimide to design membrane materials for natural gas purification and CO_2 capture. Energy Environ. Sci., 4, 201-208 (2011).

Xiao, Y.C., Chung, T.S., Guan, H.M. and Guiver, M.D., Synthesis, cross-linking and carbonization of co-polyimides containing internal acetylene units for gas separation. J. Membr. Sci., 302, 254-264 (2007).

Yu, X.W., Wang, Z., Wei, Z.H., Yuan, S.J., Zhao, J., Wang, J.X. and Wang, S.C., Novel tertiary amino containing thin film composite membranes prepared by interfacial polymerization for CO_2 capture. J. Membr. Sci., 362, 265-278 (2010).

Zhao, J., Wang, Z., Wang, J.X. and Wang, S.C., Influence of heat-treatment on CO_2 separation performance of novel fixed carrier composite membranes prepared by interfacial polymerization. J. Membr. Sci., 283, 346-356 (2006).

Zornoza, B., Seoane, B., Zamaro, J. M., Téllez C. and Coronas, J., Combination of MOFs and zeolites for mixed-matrix membranes. Chem-PhysChem, 12, 2781-2785 (2011).